STRUCTURE AND ENERGETICS OF HIGH INDEX Fe, Al, Cu AND Ni SURFACES USING EQUIVALENT CRYSTAL THEORY

Agustín M. Rodríguez
Departamento de Física
Universidad Nacional de La Plata
C.C. 67, 1900 La Plata, Argentina

Guillermo Bozzolo
Analex Corporation
3001 Aerospace Parkway
Brook Park, Ohio 44142

and

John Ferrante
National Aeronautics and Space Administration
Lewis Research Center
Cleveland, Ohio 44135

Abstract

Equivalent crystal theory (ECT) is applied to the study of multilayer relaxations and surface energies of high-index faces of Fe, Al, Ni and Cu. Changes in interplanar spacing as well as registry of planes close to the surface and the ensuing surface energies changes are discussed in reference to available experimental data and other theoretical calculations. Since ECT is a semiempirical method, we investigate the dependence of the results on the variation of the input used.

1. Introduction

In the last ten years, there has been a large number of experimental and theoretical studies on the subject of surface structure of high-index faces of metals [1-13]. Several low-energy electron diffraction (LEED) and high-energy ion scattering (HEIS) experiments provided a wealth of information, supplemented by numerous theoretical models, on the relaxation and energetics of unreconstructed metallic surfaces which, in the case of high-index faces, includes the relaxation of interlayer registries as well as interlayer spacings, where a change in the surface-parallel components of the interlayer vectors can occur without diminishing the symmetry of the surface space-group [2]. However, the number of studies on high-index faces has been limited to just a few systems (Fe(210),(211),(310) [3]; Al(210) [4],(311) [5],(331) [2] and the (311) face of Cu [6] and Ni [7]) thus providing limited information for extracting definite relaxation patterns and global behavior of such properties.

That is not the case for low-index faces: as summarized in ref. 1, several experimental techniques and almost all of the theoretical methods available have been devoted to the study of such systems. Although there is yet no simple model that fully accounts for the observed patterns in the high-symmetry cases, the available data, both experimental and theoretical, gives a good but necessarily incomplete description of general trends and patterns.

We start by discussing the (311) face of fcc metals, the fourth highest density surface, which has a relatively wide open structure. High index planes have rough contours, for which a smoothing of the electron density is likely to occur. Such density smoothing provides a driving force for interlayer registry shifts. This same argument helps to understand the relatively large contractions of the first interlayer spacing, Δd_{12}, as compared to the

corresponding values found for low-index faces, in agreement with the observation that Δd_{12} increases with surface roughness [3].

In a previous paper [12] we focused our attention on one case, Al (210), which we used both as a testing ground for the application of the theoretical framework provided by equivalent crystal theory (ECT) [13], as well as an interesting example on which we based a new concept generalizing the idea of roughness of a surface. Because of the excellent agreement with experiment found for that system, in this work we conclude our survey of multilayer relaxation studies by examining other fcc (210) surfaces with equivalent crystal theory, for those cases for which experimental data exist. We complete our study with a discussion of the structure of fcc (331) and bcc (210) and (310) surfaces.

All the reliable experimental data comes from analysis of LEED experiments. Even in this case, the values for relaxations for interlayer spacing and registry come from a rather complicated procedure. The relaxations are determined from multivariable, least squares, fits to intensity-energy curves for various beams, based on predictions from multiple scattering theory. Error estimates for the fits are based on assuming a quadratic form for deviations from the optimum r-value [4] in the minimization search in terms of the input parameters (i.e., layer spacing and registry, potential parameters and Debye temperature). The error bars attached to the experimental results for the relaxations thus included information from changes in the input parameters of the multiple scattering model as well as errors inherent to the experimental technique used. In this work we address a similar issue, by defining the uncertainties in the optimum relaxation values obtained from an energy search, by including a margin of error in our theoretical predictions that, in the particular case of semiempirical methods such as ECT, can be attributed to fluctuations in the input

data used (generally experimentally determined).

The paper is organized as follows: in section 2 we briefly discuss equivalent crystal theory and provide the essential working equations. Section 3 focuses on the case of perpendicular relaxations of low-index faces in order to illustrate the need for the introduction of theoretical 'error bars', thus providing a better framework for comparison between experimental and theoretical results. In section 4 we apply ECT to several fcc high-index metallic surfaces and compare with experimental values when available. Conclusions are drawn in section 5.

2. Equivalent Crystal Theory

Equivalent crystal theory [13] is based on an exact relationship between the total energy and atomic locations and applies to surfaces and defects in both simple and transition metals as well as in covalent solids. Lattice defects and surface energies are determined via perturbation theory on a fictitious, equivalent single crystal whose lattice constant is chosen to minimize the perturbation. The energy of the equivalent crystal, as a function of its lattice constant is given by a universal binding energy relation [14].

Let ε be the total energy to form the defect or surface, then $\varepsilon = \sum_i \varepsilon_i$ where ε_i is the contribution from an atom i close to the defect or surface. ECT is based on the concept that there exists, for each atom i, a certain perfect, equivalent crystal with its lattice parameter fixed at a value so that the energy of atom i in the equivalent crystal is also ε_i. This equivalent crystal differs from the actual ground-state crystal only in that its lattice constant may be different from the ground-state value. We compute ε_i via perturbation theory, where the perturbation arises from the difference in the ion core electronic potentials of the actual defect solid and those of the effective bulk single crystal.

For the sake of simplicity, the formal perturbation series is approximated by simple, analytic forms which contain a few parameters, which can be calculated from experimental results or first-principles calculations. Our simplified perturbation series for ε_i is of the form

$$\varepsilon_i = \Delta E \left\{ F^* \left[a_1^*(i)\right] + \sum_j F^* \left[a_2^*(i,j)\right] + \sum_{j,k} \left[a_3^*(i,j,k)\right] + \sum_{p,q} F^* \left[a_4^*(i,p,q)\right] \right\} \qquad (1)$$

where $F^*[a^*] = 1 - (1 + a^*)e^{-a^*}$ and ΔE is the cohesive energy. In this expression, we distinguish four different contributions to the energy of atom i and thus, the existence of four different equivalent crystals which have to be determined for each atom i.

The first term, $F^*\left[a_1^*(i)\right]$, contributes when average neighbor distances are altered via defect or surface formation. It can be thought of as representing local atom density changes. In most cases, this 'volume' term is the leading contribution to ε_i and in the case of isotropic volume deformations, it gives ε_i to the accuracy of the universal energy relation [14]. The value of $a_1^*(i)$, the lattice parameter of the first equivalent crystal associated with atom i, is chosen so that the perturbation (the difference in potentials between the solid containing the defect and its bulk, ground-state equivalent crystal) vanishes. Within the framework of ECT, this requirement translates into the following condition from which $a_1^*(i)$ is determined:

$$N R_1^p e^{-\alpha R_1} + M R_2^p e^{-(\alpha + \frac{1}{\lambda})R_2} - \sum_{defect} r_j^p e^{-[\alpha + S(r_j)]r_j} = 0 \qquad (2)$$

where the sum over the defect crystal or surface is over all neighbors within second-neighbor (NNN) distance. r_j is the actual distance between atom i and a neighbor atom j, N and M are the number of nearest-neighbor (NN) and next-nearest-neighbors, respectively, of the equivalent crystal (12 and 6 for fcc, 8 and 6 for bcc) and p, α and λ are parameters known for each atomic species, listed in Table 1. $S(r_j)$ is a screening function and R_1

and R_2 are the NN and NNN distances in the equivalent crystal. The equivalent lattice parameter, a_1, is thus related to the scaled quantity a_1^* via $a_1^* = \left(\frac{R_1}{c} - r_{WSE}\right)/l$, where r_{WSE} is the equilibrium Wigner-Seitz radius, l is a scaling length and c is the ratio between the equilibrium lattice constant and r_{WSE}.

The higher-order terms are relevant for the case of anisotropic deformations. The linear independence attributed to these four terms is consistent with the limit of small perturbations which we assume for the formulation of ECT. The second term, $F^*[a_2^*(i,j)]$, is a two-body term which accounts for the increase in energy when NN bonds are compressed below their equilibrium value. This effect is also modeled with an equivalent crystal, whose lattice parameter is obtained by solving a perturbation equation given by

$$N R_1^p e^{-\alpha R_1} - N R_0^p e^{-\alpha R_0} + A_2 R_0^p \sum_j (R_j - R_0) e^{-\beta(R_j - R_0)} = 0, \tag{3}$$

where $\beta = 4\alpha$ for the metals used in this work, and R_1 is the NN distance of the equivalent crystal associated with the deviation of NN bond length R_j from R_0, and R_0 is the bulk NN distance at whatever pressure the solid is maintained (generally, R_0 is the ground-state, zero-pressure value). A_2 is a constant determined for each metal (see Table 1 for a list of values of A_2 used in this work). The scaled equivalent lattice parameter is then $a_2^* = \left(\frac{R_1}{c} - r_{WSE}\right)/l$.

The third term, $F^*[a_3^*(i,j,k)]$ accounts for the increase in energy that arises when bond angles deviate from their equilibrium values of the undistorted single crystal. This is a three-body term and the equivalent lattice parameter associated with this effect is obtained from the perturbation equation

$$N R_1^p e^{-\alpha R_1} - N R_0^p e^{-\alpha R_0} + A_3 R_0^p e^{-\alpha(R_j + R_k - 2R_0)} \sin(\theta_{jk} - \theta) = 0 \tag{4}$$

where A_3 is a constant listed in Table 1 and θ_{jk} is the angle between the NN distances R_j and R_k with the atom i at the center. θ is the equilibrium angle, 70.5 degrees for bcc and 90 degrees for fcc. This term contributes only when there is a bond-angle anisotropy ($\theta_{jk} \neq \theta$). The scaled lattice parameter is then $a_3^* = \left(\frac{R_1}{c} - r_{WSE}\right)/l$.

The fourth term, $F^*\left[a_4^*(i,p,q)\right]$, describes face diagonal anisotropies (see Ref. 13 for a detailed description, for each lattice type, of the structural effect associated with this term). The perturbation equation reads

$$N R_1^p e^{-\alpha R_1} - N R_0^p e^{-\alpha R_0} + A_4 R_0^p \frac{|d_p - d_q|}{d} e^{-\alpha(R_j+R_k+R_l+R_m-4R_0)} = 0 \qquad (5)$$

where d is the face diagonal of the undistorted cube and A_4 is a constant adjusted to reproduce the experimental shear elastic constants (Table 1). Finally, $a_4^* = \left(\frac{R_1}{c} - r_{WSE}\right)/l$.

Consider a rigid surface (i.e., no interlayer relaxation): all bond lengths and angles retain their bulk equilibrium values, thus $F^*(a_2^*) = F^*(a_3^*) = F^*(a_4^*) = 0$. The surface energy is therefore obtained by solving for the 'volume' term represented by $F^*(a_1^*)$ only. If we consider a rigid displacement of the surface layer towards the bulk, as is the case in most metallic surfaces, the higher-order terms become finite: some bonds are compressed, contributing to $F^*(a_2^*)$, the bond angles near the surface are distorted as well as the difference between face diagonals in some cases, generating an increase of energy via $F^*(a_3^*)$ and $F^*(a_4^*)$. For the case studied in this work, these additional contributions to ε_i are generally small, representing only 1 % to 2 % of the total energy. However, while these anisotropy terms are small for metals when there is no reconstruction, they play an important role in the energetics of these defects where the differences in energy between the rigid and relaxed configurations are also small.

3. Multilayer relaxation of pure crystals

Before proceeding to the calculation of multilayer relaxation in high-index faces, we will discuss some features of theoretical calculations of these quantities. Ref. 1 provides a reasonably large sample of both experimental and theoretical results for changes in interlayer spacing in pure fcc and bcc crystals. In all cases, the semiempirical, theoretical techniques used rely either on input data (generally experimentally determined) or on certain approximations for some of the variables of relevance. Necessarily, results will depend on such choices. Multilayer relaxations involve at best very small changes in position, and correspondingly, comparable changes in surface energy, whose minimization is the criterion used to determine the final interlayer spacings. Thus, the search for a minimum of the surface energy, as accurate as the minimization technique might be, will be strongly influenced by the two factors indicated above: the approximations used and the shallowness of the minimum in the surface energy surface resulting from small changes in the input parameters. As a consequence, to quote just one value for each of the changes in interlayer spacings as is ordinarily done, might not reflect the ambiguities in these calculations. In this paper we adopt a different path: to each theoretical prediction, we will attach an estimate of the possible errors due to any of the reasons mentioned above. Although there is no certain way to determine such errors (after all, the predictions are, within their own framework, exact), we will see that changes on the order of 1 % in the surface energy can generate quite interesting variations in the relaxation schemes predicted. In particular, within the framework of ECT, such small changes in the surface energy can be easily obtained by changing any of the input parameters (lattice constant, cohesive energy, bulk modulus) by a similar amount, well below the usual experimental errors in the determination of such quantities.

To illustrate this issue, we will focus our attention on the surface structure of some fcc pure metals (Al, Au, Cu and Ni). As can be seen in Tables 2-11 of ref. 1, previous theoretical and experimental studies show a wide spread in the predictions of the changes in interlayer spacings for the (100) and (110) surfaces. Even results obtained within the same theoretical technique (embedded atom method (EAM), ECT) do not agree with each other (due to different fitting procedures of the embedding function in the case of EAM and different input data in both cases). Although there is general qualitative agreement, regarding the contraction or expansion pattern found for successive layers, in some cases the absolute theoretical values show poor agreement with experimental results (see, for example, Al (100)). The ECT results (from refs. 1 and 13) also highlight this inconsistency. The difference between the values obtained in this work and those from previous applications of ECT is easily traceable to slightly different values of some of the input parameters.

As mentioned above, in order to account for these and other ambiguities in the calculation, we investigated the change in predicted relaxations due to small changes in the rigid surface energy. We thus defined 'error bars' in such way that all the intermediate values so obtained predict variations in surface energies within that tolerance. Needless to say, this range of values does not include all the possible sets (Δd_{12}, Δd_{23}) that correspond to surface energies within the allowed values. It is interesting to note, however, that in most cases, all the experimental as well as theoretical predictions fall within the range of uncertainties in such procedure.

It should be noted that when comparing our theoretical predictions with available experimental results, the error bars quoted in each case are similar in that the optimum relaxations are determined by minimization of some property by varying the input parame-

ters. To illustrate this point, we first discuss the surface energies and multilayer relaxations of the unreconstructed low-index surfaces of pure Al, Ni, Cu and Au crystals. In Table 2 we display the ECT predictions for the surface energies and compare the results with typical experimental values for polycrystalline samples [15,16]. The agreement is excellent in all cases. We note that experimental values for the surface energies are for polycrystalline surfaces, thus could be strongly dominated by the predominant surface plane.

In table 3 we compare results for the multilayer relaxations of the first two interlayer spacings for those cases for which recent experimental data is available [16-24]. Once again the agreement is excellent, as it was shown in previous ECT studies of surface structure [1]. The inclusion of the theoretical 'error bar', as mentioned above, allows for a better comparison with experiment as it shows that for most cases, small changes in the input parameters of the method suffice to account for the whole range of possible experimental results. The exceptions are Al(100) and Al(111), where the outward relaxation of the surface layer has been attributed to an electron promotion effect [17]. Semiempirical methods (ECT, EAM. etc.), unless specifically designed to do so, do not generally allow for such fine electronic structure effects, thus it is not surprising that our results for Δd_{12} in these cases predict surface layer contractions, even when the 'error bar' is taken into account. For completeness we also include results for the surface relaxation when only the top plane is allowed to relax, in order to single out correlations with subsequent interlayer spacing changes on the surface plane. Again, the agreement with available experimental data is very good in all cases.

4. Multilayer relaxation of high-index surfaces

We now discuss the application of ECT to the study of the surface structure of high-

index faces of fcc (Al, Cu, Ni) and bcc (Fe) metals. For each case, we computed the changes in interlayer spacing for the top six layers as well as the changes in registry. We follow the notation used in previous work on similar systems [2-7]. As discussed in Section 1 and 3, in this work we focus our attention not only on the absolute values of the relaxations, as obtained from experiment and predicted by the theory, but in the associated uncertainties as well. Although this last issue could be of importance when comparing the quality of the predictions, the main reason why it is highlighted here is to indicate the influence of external variables on the final results. We believe that because of the nature of the procedure used to perform the LEED analysis on the one hand, and the inherent uncertainties brought on by the simplifications adopted in designing semiempirical techniques, a thorough discussion of the results would not be complete if this issue was not appropriately addressed. In this spirit, figs. 1-4 summarize the ECT results for several fcc and bcc systems and the corresponding LEED results for those cases for which experimental results are available. We have chosen this format for presenting the data for ease of comparison of experiment with theory. Fig. 1 displays results for Al faces. Al (210) and (331) display a similar behavior: large relaxation of the first interlayer spacing, followed by a comparable contraction of the second layer and an expansion of the third. The corresponding changes in registry are at best too small to definitely predict a trend in either case. As discussed in a previous application of ECT to Al (210) [12], the ECT results give a final configuration of higher symmetry and optimized 'coverage' of the space between atoms in the top layer. Whereas both theory and experiment agree in the case of registry changes in that the trends are the same and there is substantial overlap of the error bars, the agreement is less noticeable for the perpendicular relaxations, although the theoretical error bars clearly indicate that only

small changes of the input parameters are needed to improve the quantitative agreement. Fig. 2 shows similar results for fcc (311) surfaces for Al, Cu and Ni. The trends found in the LEED results for Δd_{12} are reproduced by ECT in all three cases. Although there are seemingly poorer results for the other relaxations, the principal point in this paper is that small shifts in the input parameters in the semiempirical method can bring trends into agreement. In the case of Ni(311), for which experimental values have been reported [7], there is good agreement with the associated registry changes. For completeness, we include the ECT results for Ni and Cu (210) (fig. 3), although there is no experimental data available for comparison. In spite of the differences in electronic structure, both metals display an almost identical behavior regarding the structure of the surface, which, together with the Al (210) results displayed in Fig. 1.a, indicate a defined relaxation pattern for such fcc faces.

We conclude the presentation of results with a bcc system, Fe, for which several studies have been carried out. Fig. 4 displays LEED [3] and ECT results for Fe (210) and (310) surfaces. As expected, the percentage change in interplanar spacings is much larger for bcc metals than for fcc, a feature clearly reproduced by ECT. The contraction-expansion pattern is also generally reproduced for both parallel and perpendicular relaxations. For completeness, we include the numerical results for all the cases studied in this paper in tables 4-7. Table 4 displays the results for the (210), (311) and (331) surfaces of Al where the error bars are related to changes of just 1 % in the surface energy. Table 5 and 6 show the results for the (311) and (210) faces of Ni and Cu, respectively.

5. Conclusions

In conclusion, in this paper we have used equivalent crystal theory to examine relax-

ations in higher index planes of Al, Cu, Ni and Fe where both perpendicular and parallel surface relaxations can occur and there is experimental data available for comparison. In addition, we attempt to raise questions regarding the nature of agreement between theory and experiment in that the success of theoretical agreement has been based on trends and absolute values of specific relaxations. Since semiempirical theoretical methods involve the use of experimental input parameters and conclusions are based on small changes in lattice geometry, we test the sensitivity of our predictions to small variations in input parameters. We find that in most cases, agreement involving trends can be greatly improved by small changes in these parameters and that careful consideration must be given to the method of making comparisons.

Acknowledgments

Fruitful discussions with Dr. N. Bozzolo are gratefully acknowleged. This work was partially supported by the Engineering Directorate, NASA Lewis Research Center. A.M.R. would like to thank the Ohio Aerospace Institute, for partial financial support and the N.A.S.A. Lewis Research Academy, where part of this work was done.

References

[1]A. M. Rodríguez, G. Bozzolo and J. Ferrante, Surf. Sci. **289** (1993) 100, and references therein.

[2]D. L. Adams and C. Sørensen, Surf. Sci. **166** (1986) 495.

[3]J. Sokolov, F. Jona and P. M. Marcus, Phys. Rev. B **29** (1984) 5402; *ibid.*, Solid State Commun. **49** (1984) 307; *ibid.*, Phys. Rev. B **31** (1984) 1929; J. Sokolov, H. D. Shih, U. Bardi, F. Jona and P. M. Marcus, J. Phys. C (Solid State Phys.) **17** (1984) 371.

[4]D. L. Adams, V. Jensen, X. F. Sun and J. H. Vollesen, Phys. Rev. B **38** (1988) 7913.

[5]J. R. Noonan, H. L. Davis and W. Erley, Surf. Sci. **152/153** (1985) 142.

[6]P. R. Watson and K. A. R. Mitchell, Surf. Sci. **203** (1988) 323; R. W. Streater, W. T. Moore, P. R. Watson, D. C. Frost and K. A. R. Mitchell, Surf. Sci. **72** (1978) 744.

[7]D. L. Adams, W. T. Moore and K. A. R. Mitchell, Surf. Sci. **149** (1985) 407; W. T. Moore, S. J. White, D. C. Frost and K. A. R. Mitchell, Surf. Sci. **116** (1982) 253; J. B. Pendry, J. Phys. C (Solid State Phys.) **13** (1980) 937.

[8]P. Jiang, P. M. Marcus and F. Jona, Solid State Commun. **59** (1986) 275.

[9]P. Jiang, F. Jona and P. M. Marcus, Phys. Rev. B **35** (1987) 7952.

[10]J. S. Luo and B. Legrand, Phys. Rev. B **38** (1988) 1728.

[11]S. B. Sinnot, M. S. Stave, T. J. raeker and A. E. DePristo, Phys. Rev. B 44 (1991) 8927.

[12]A. Rodríguez, G. Bozzolo and J. Ferrante, to be published.

[13]J. R. Smith and A. Banerjea, Phys. Rev. Lett. **59** (1987) 2451; *ibid.*, Phys. Rev. B**37** (1988) 10411; J. R. Smith, T. Perry, A. Banerjea, J. Ferrante and G. Bozzolo, Phys. Rev. B44 (1991) 6444.

[14]J. H. Rose, J. Ferrante and J. R. Smith, Phys. Rev. Lett. **47** (1981) 675.

[15]W. R. Tyson, J. Appl. Phys. **47** (1976) 459.

[16]W. R. Tyson and W. A. Miller, Surf. Sci. **62** (1977) 267.

[17]P. J. Feibelman, Phys. Rev. B **46** (1992) 2532.

[18]H. L. Davis, J. B. Hannon, K. B. Ray and E. W. Plummer, Phys. Rev. Lett. **68** (1992) 2632.

[19]J. R. Noonan and H. L. Davis, Phys. Rev. B29 (1984) 4349.

[20]J. R. Noonan and H. L. Davis, J. Vac. Sci. Technol. A8 (1990) 2671.

[21]J. W. M. Frenken, J. F. van der Veen and G. Allan, Phys. Rev. Lett. **51** (1983) 1876.

[22]S. M. Yalisove, W. R. Graham, E. D. Adams, M. Copel and T. Gustafsson, Surf. Sci. **171** (1986) 400.

[23]J. E. Demuth, P. M. Marcus and D. W. Jepsen, Phys. Rev. **11** (1975) 1460.

[24]R. Mayer, C. Zhang, K. G. Lynn, W. E. Frieze, F. Jona and P. M. Marcus, Phys. Rev. B35 (1987) 3102.

[25]I. Stensgaard, R. Feidenhans'l and J. E. Sorensen, Surf. Sci. **128** (1983) 281.

[26]S. A. Lindgren, L. Wallden, J. Rundgren and P. Westrin, Phys. Rev. B29 (1984) 576.

TABLE 1: COMPUTED CONSTANT AND EXPERIMENTAL INPUT FOR ECT

[The constant p is $2n-2$, where n is the atomic principal quantum number, l (in Å) is a scaling length and λ (in Å) is a screening parameter (see text). The constants A_3 and A_4 are dimensionless. ΔE (in eV) is the cohesive energy and a_e (in Å) the equilibrium lattice constant.]

Element	p	l	α	λ	$10^{-2}A_2/D$	$10^{-1}A_4/D$	$10^{-4}D$	ΔE	a_e
Al	4	0.336	2.105	0.944	7.822	2.104	591.4	3.34	4.05
Cu	6	0.272	2.935	0.765	5.784	2.530	99.74	3.50	3.615
Ni	6	0.270	3.015	0.759	7.382	2.793	100.1	4.435	3.524
Fe	6	0.277	3.124	0.770	9.183	1.887	60.62	4.29	2.86

TABLE 2: EXPERIMENTAL (Exp.) AND
RELAXED ECT SURFACE ENERGIES
OF Al, Cu, Ni AND Au

[In ergs/cm^2.]

Technique	Al	Cu	Ni	Au
Exp. [15]	1200	1790	2270	1560
Exp. [16]	1140	1780	2380	1500
Exp. [16]	1180	1770	2240	1540
ECT(100)	1203	2309	2982	1546
ECT(110)	1284	2373	3073	1621
ECT(111)	856	1767	2274	1136

TABLE 3: SURFACE RELAXATIONS OF Al, Cu AND Ni AS PERCENTAGES OF THE
BULK INTERPLANAR SPACINGS

[The ECT Δd_{12} column displays results for relaxations of the top layer only while the ECT (two layers) columns display results for the case when the top two layers are allowed to relax.]

Element	Face	Experiment			ECT	ECT	(two-layers)
		Δd_{12}	Δd_{23}	Ref.	Δd_{12}	Δd_{12}	Δd_{23}
Al	(100)	+1.8		[18]	-4.68±1.62	-5.05±1.58	+3.35±0.80
	(110)	-8.5±1.0	+5.5±1.1	[19]	-8.29±2.35	-9.53±3.58	+1.90±2.24
	(111)	+1.7±0.3	+0.5±0.7	[20]	-3.67±1.21	-3.94±1.19	+2.75±0.61
Ni	(100)	-3.2±0.5		[21]	-3.53±1.68	-3.82±1.68	+2.48±0.85
	(110)	-9.0±1.0	+3.5±1.5	[22]	-6.32±2.44	-6.55±3.63	+0.34±2.24
	(111)	-1.2±1.2		[23]	-2.89±1.29	-3.10±1.25	+2.12±0.63
Cu	(100)	-2.1	+0.45	[24]	-3.52±1.74	-3.81±1.70	+2.47±0.86
	(110)	-7.5±1.5	+2.5±1.5	[25]	-6.31±2.46	-6.51±3.83	+0.29±2.44
	(111)	-0.7±0.5		[26]	-2.88±1.30	-3.10±1.25	+2.12±0.63

TABLE 4: PERPENDICULAR (Δd) AND PARALLEL (Δa) RELAXATIONS OF Al (210), (311) AND (331) SURFACES EXPRESSED AS PERCENTAGES OF THE CORRESPONDING BULK SPACINGS

	Al (210)	Al (311)	Al (331)
Δd_{12}	-8.08±4.44	-8.88±2.88	-4.17±4.17
Δd_{23}	-7.07±3.82	-0.04±2.77	-4.52±3.47
Δd_{34}	+2.90±4.23	-2.42±4.36	+6.08±3.59
Δd_{45}	-3.36±5.83	+5.05±5.25	-3.56±4.97
Δd_{56}	+4.21±6.84	-1.96±4.92	+3.36±5.95
Δa_{12}	-0.20±2.42	+0.87±2.67	-2.65±2.26
Δa_{23}	+0.02±2.60	+0.53±3.19	+0.02±2.63
Δa_{34}	+0.79±2.90	-0.81±4.09	-0.08±3.08
Δa_{45}	+0.04±3.49	+2.27±3.86	+1.87±3.64
Δa_{56}	-0.47±4.42	-0.37±4.96	-1.41±3.76

TABLE 5: PERPENDICULAR (Δd) AND PARALLEL (Δa) RELAXATIONS OF Ni (210) AND (311) SURFACES EXPRESSED AS PERCENTAGES OF THE CORRESPONDING BULK SPACINGS

	Ni (210)	Ni (311)
Δd_{12}	-4.54±5.04	-5.57±3.26
Δd_{23}	-4.96±4.15	-0.77±3.00
Δd_{34}	+1.06±4.37	-1.61±4.32
Δd_{45}	-1.96±5.76	+4.11±5.01
Δd_{56}	+3.17±6.73	-1.41±5.00
Δa_{12}	0.00±2.42	+0.53±2.80
Δa_{23}	+0.03±2.55	+0.46±3.10
Δa_{34}	+0.46±2.78	-0.52±3.92
Δa_{45}	+0.15±3.38	+0.53±4.89
Δa_{56}	-0.45±4.12	-0.31±4.58

TABLE 6: PERPENDICULAR (Δd) AND PARALLEL (Δa) RELAXATIONS OF Cu (210) AND (311) SURFACES EXPRESSED AS PERCENTAGES OF THE CORRESPONDING BULK SPACINGS

	Cu (210)	Cu (311)
Δd_{12}	-4.48±5.07	-5.54±3.27
Δd_{23}	-4.91±4.17	-0.81±2.99
Δd_{34}	+0.96±4.38	-1.75±4.33
Δd_{45}	-2.03±5.80	+4.32±5.05
Δd_{56}	+3.20±6.80	-1.60±5.02
Δa_{12}	0.00±2.43	+0.55±2.79
Δa_{23}	+0.05±2.55	+0.50±3.12
Δa_{34}	+0.48±2.82	-0.54±4.00
Δa_{45}	+0.11±3.49	+0.50±5.08
Δa_{56}	-0.50±4.31	-0.30±4.73

TABLE 7: PERPENDICULAR (Δd) AND PARALLEL (Δa) RELAXATIONS OF Fe (210) AND (310) SURFACES EXPRESSED AS PERCENTAGES OF THE CORRESPONDING BULK SPACINGS

	Fe (210)	Fe (310)
Δd_{12}	-7.65±7.06	-30.45±1.99
Δd_{23}	-2.81±5.48	+15.5±1.83
Δd_{34}	-4.53±4.84	-19.82±1.91
Δd_{45}	+0.06±5.14	+11.49±1.81
Δd_{56}	+1.00±4.30	
Δa_{12}	+2.37±2.12	-2.36±1.47
Δa_{23}	+3.10±2.05	+6.36±1.67
Δa_{34}	+1.47±2.70	-4.82±1.92
Δa_{45}	-0.75±2.70	+2.60±1.93
Δa_{56}	+0.40±3.23	

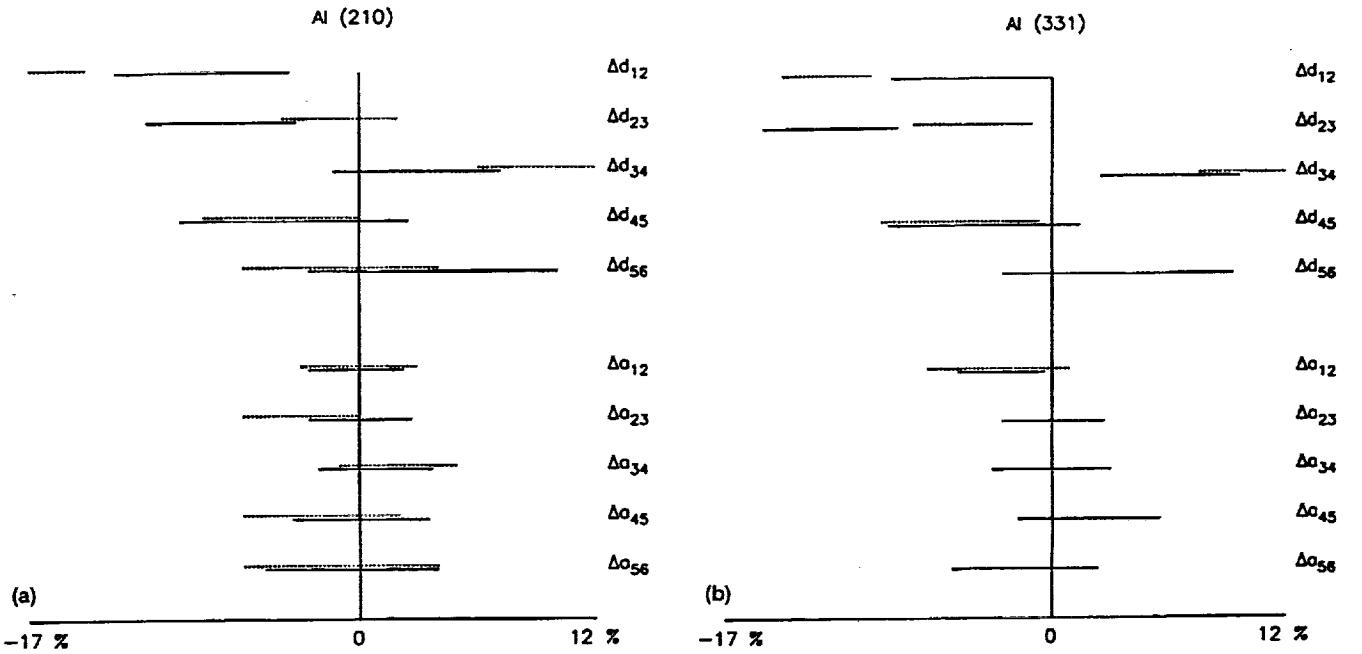

Figure 1.—Theoretical (solid line) and experimental (dotted line or solid squares) values for the perpendicular (Δd) and parallel (Δa) relaxations for (a) Al(210) and (b) Al(331), expressed as percentages of the corresponding bulk spacings. The experimental values were taken from refs. 4 and 2, respectively.

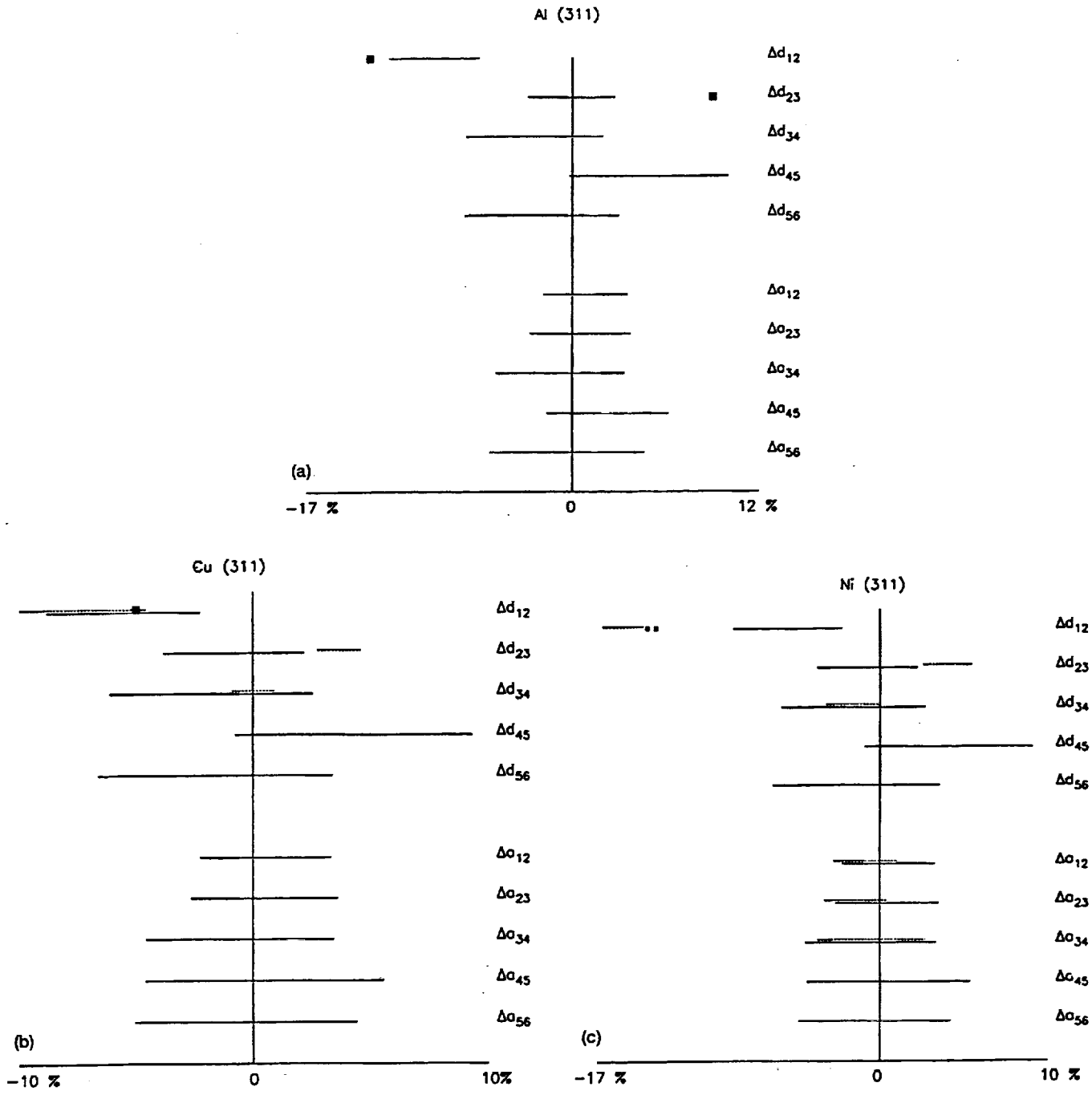

Figure 2.—Theoretical (solid line) and experimental (dotted line or solid squares) values for the perpendicular (Δd) and parallel (Δa) relaxations for the (311) face of (a) Al, (b) Cu and (c) Ni, expressed as percentages of the corresponding bulk spacings. The experimental values were taken from refs. 5, 6 and 7, respectively.

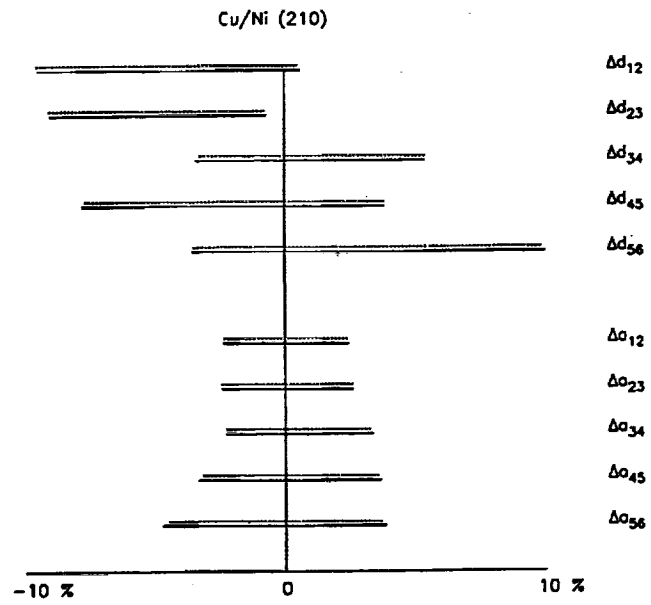

Figure 3.—Theoretical values for the perpendicular (Δd) and parallel (Δa) relaxations for the (210) face of Cu (solid line) and Ni (dotted line), expressed as percentages of the corresponding bulk spacings.

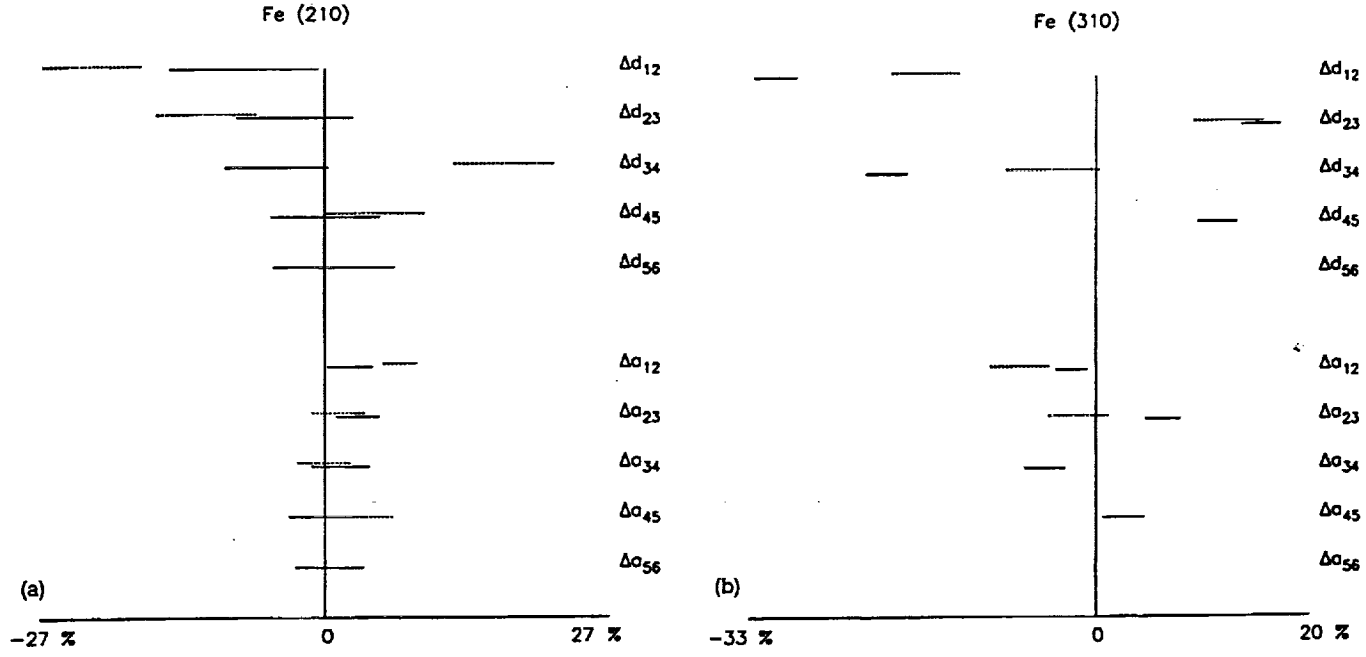

Figure 4.—Theoretical (solid line) and experimental (dotted line) [3] values for the perpendicular (Δd) and parallel (Δa) relaxations for the (a) (210) and (b) (310) faces of Fe, expressed as percentages of the corresponding bulk spacings.